



OPEN

Multiparametric ultrasound findings in acute kidney failure due to rare renal cortical necrosis

Paul Spiesecke¹, Frédéric Münch², Thomas Fischer¹, Bernd Hamm¹ & Markus H. Lerchbaumer¹✉

Renal cortical necrosis (RCN) is a rare cause of acute kidney failure and is usually diagnosed on the basis of characteristic enhancement patterns on cross-sectional imaging. Contrast-enhanced ultrasound (CEUS) offers benefits in patients with kidney failure in the clinical setting including the use of a nonnephrotoxic intravascular contrast agent and the fact that it can be performed at the bedside in critical cases. Therefore, the aim of this study is to investigate whether CEUS can reliably identify typical imaging features of RCN. We retrospectively analyzed 12 patients with RCN examined in our department and confirmation of the diagnosis by either histopathology, other contrast-enhanced cross-sectional imaging tests, and/or CEUS follow-up. Assessed parameters in conventional US were reduced echogenicity, loss of corticomedullary differentiation, length and width of kidney, hypoechoic rim, resistance index and in CEUS delayed wash-in of contrast agent (> 20 s), reverse rim sign, maximum nonenhancing rim and additional renal infarction. Furthermore, imaging features in RCN were compared with the findings in renal vein thrombosis (RVT), among them echogenicity, corticomedullary differentiation, hypoechoic rim, RI value, delayed cortical enhancement, total loss of cortical perfusion and enhancement of renal medulla. All 12 patients showed the reverse rim sign, while a hypoechoic subcapsular rim was only visible in four patients on B-mode ultrasound. A resistance index (RI) was available in 10 cases and was always less than 1. RI was a strong differentiator in separating RVT from RCN (RI > 1 or not measurable due to hypoperfusion as differentiator, $p = 0.001$). CEUS showed total loss of medullary enhancement in all cases of RVT. With its higher temporal resolution, CEUS allows dynamic assessment of renal macro- and microcirculation and identification of the typical imaging findings of RCN with use of a nonnephrotoxic contrast agent.

Abbreviations

ADPKD	Autosomal-dominant polycystic kidney disease
ANCA	Anti-neutrophil cytoplasmic antibody
CCDS	Color-coded duplex sonography
ceCT	Contrast-enhanced computed tomography
ceMRI	Contrast-enhanced magnetic resonance imaging
CEUS	Contrast-enhanced ultrasound
NSF	Nephrogenic systemic fibrosis
PW	Pulsed wave
RCN	Renal cortical necrosis
RI	Resistance index
RPGN	Rapid progressive glomerulonephritis
RVT	Renal vein thrombosis
US	Ultrasound

Renal cortical necrosis (RCN) is a rare cause of acute renal failure and is more prevalent in developing countries with inadequate healthcare systems¹. In acute RCN, both the glomeruli and tubules become necrotic, while

¹Department of Radiology, Charité - Universitätsmedizin Berlin, Corporate Member of Freie Universität Berlin, Humboldt-Universität Zu Berlin, Campus Charité Mitte, Charitéplatz 1, 10117 Berlin, Germany. ²Department of Nephrology and Intensive Care Medicine, Charité - Universitätsmedizin Berlin, Corporate Member of Freie Universität Berlin, Humboldt-Universität Zu Berlin, Berlin, Germany. ✉email: markus.lerchbaumer@charite.de

acute tubular necrosis only affects the tubules². Fibrin thrombi in the renal capillaries have been described as a pathologic correlate of RCN². Fogo et al. visualized the coagulative necrosis in histopathologic examples³.

While the pathogenesis remains unclear and may be multifactorial, small case series or case reports describe an association with shock, sepsis, and postpartum hemorrhage, which lead to reduced renal arterial blood flow secondary to vascular spasm, microvascular injury, or intravascular coagulation^{4–6}. Acute renal failure due to RCN appears to be more common in infants and in perinatal women¹.

In a case series, Frimat et al. describe the clinical course of 18 patients with RCN due to postpartum hemorrhage⁷. All of the included patients were in need of hemodialysis since acute renal failure developed quickly⁷. Eventually, in all of the patients RCN converged in chronic kidney disease, whereas 6 months postnatal 8/18 patients still were in need of hemodialysis⁷.

Histologically, renal cortical necrosis may affect the whole cortex with or without the medulla or just its subcapsular parts. The necrosis and organ damage is described as irreversible loss of function and poor prognosis⁶.

RCN has typical features that can be demonstrated by cross-sectional imaging such as contrast-enhanced computed tomography (ceCT) and contrast-enhanced magnetic resonance imaging (ceMRI) including a non-enhancing cortical rim that correlates with the histopathological findings⁸. Nonenhancement of the cortical rim with simultaneous enhancement of the renal medulla is characteristic of RCN and is known as the “reverse rim sign”^{9,10}. This must not be confused with the “cortical rim sign”, which describes a very thin edge of enhancing, viable renal cortex supplied by collaterals of capsular arteries^{9,10}. Nevertheless, biopsy and histopathological examination remain the gold standard in confirming the diagnosis of acute RCN and assessing the extent of vascular damage and identifying the affected renal structures¹¹.

Ultrasound (US) with color-coded duplex sonography (CCDS) is the primary imaging technique to assess macrovascularization of renal transplants in the early post-transplant period but has been demonstrated to be especially highly specific for macrovascular problems such as renal artery stenosis or vein thrombosis^{12,13}. Contrast-enhanced ultrasound (CEUS) is increasingly being used for evaluation of organ perfusion and lesion characterization, as advocated by the EFSUMB guidelines. Specifically, the guidelines recommend CEUS for differentiating cortical necrosis from renal infarction¹⁴. Real-time dynamic CEUS depicts microcirculation throughout the kidney and should therefore identify the reverse rim sign to diagnose acute RCN. So far, just a few case reports and the results of a single-center investigation of CEUS in acute RCN in five patients have been published¹⁵. Thus, the aim of our study is to evaluate CEUS imaging findings in acute RCN in both native kidneys and renal transplants in adult patients.

Material and methods

Study cohort. All patients gave written informed consent to anonymized use of their data prior to imaging. This is part of the routine clinical procedure at our department. This retrospective analysis is registered at the local ethical committee of our institution (Ethikkommission der Charité-Universitätsmedizin Berlin, EA1/320/20). All study data were collected in compliance with the principles expressed in the 2002 Declaration of Helsinki. Figures were arranged considering anonymization in order to avoid their affiliation to patient's identity.

The retrospective analysis included patients who underwent CEUS in our department from 2009 to 2019. Inclusion criteria were: (1) CEUS examination with documentation of sufficient image data and detailed written report of findings, (2) diagnosis of renal cortical necrosis in CEUS, (3) available clinical data, (4) patient age ≥ 18 years, and (5) diagnosis confirmed by biopsy and histopathology or imaging follow-up by either CEUS, ceCT, or ceMRI (in case of cross-sectional imaging one month before or after index examination and in case of CEUS follow-up within 2 months after index examination). Exclusion criteria were: (1) substandard image quality, (2) no clinical data available, (3) no imaging follow-up and missing histopathological confirmation, and (4) proven renal vein thrombosis at the time of index examination.

Using the radiology information system (RIS), we collected the following clinical information: renal or systemic primary disease, oliguria, fever, hypertonia, anemia, secondary hyperparathyroidism, diabetes mellitus, and creatinine value determined closest to the time of the index CEUS examination. Furthermore, the included cases were assessed regarding occurrence of acute RCN in the postpartum period or after renal transplant.

US and CEUS examination protocol. Gray-scale B-mode imaging of the kidney or kidney transplant was performed using a convex array transducer to assess renal size, echogenicity, and homogeneity.

Standardized CCDS was performed to assess venous outflow and arterial circulation and to calculate resistance indices (RI) for different segmental arteries at the pyeloparenchymal border (generally as a mean value of three measured RI in the upper, middle and lower third of the kidney). Power Doppler imaging was used to identify focal perfusion loss.

CEUS examinations were performed as part of clinical routine using high-end ultrasound systems (Aplio 500/i900, Canon Medical Systems Corporation, Tochigi, Japan; Acuson Sequoia/S3000, Siemens Healthineers, Mountain View, CA, USA; GE Logiq E9, GE Healthcare, Chicago, Illinois, USA) with state-of-the-art CEUS-specific protocols available at the time of examination. All convex transducers employed in study patients were required to be for abdominal use with a frequency range of 1–6 MHz. The very-low-mechanical-index (< 0.1) technique was used to avoid early microbubble destruction. A bolus of 1.2–1.6 mL of ultrasound contrast agent (SonoVue, Bracco Imaging, Milan, Italy) was injected up to three times, if necessary, for example to assess arterial inflow in both kidneys. Following contrast agent injection, the kidney or renal transplant was scanned for at least five minutes to capture the wash-in phase (cine loop of 30 to 45 s) and late contrast phase between two and 5 min after injection of contrast agent. Baseline B-mode US, CCDS, and CEUS were reviewed by a highly

experienced radiologist with more than 10 years of experience in CEUS imaging (EFSUMB level 3) in consensus with a second experienced radiologist.

Cross-sectional imaging. Additional multiphase ceCT examinations (arterial and venous/delayed phase) were performed in a 64–128 detector CT scanner using a standard protocol. The contrast agent was bolus-injected into an antecubital vein at a flow rate of 3.0–4.5 mL/s. Contrast media with an iodine concentration of 350–400 mg/mL were administered and their amount adopted to patient's body weight, followed by a 50 mL saline flush. The acquisition direction was craniocaudal.

CeMRI was performed at 1.5 T or 3.0 T using phased-array body coils. The imaging protocols comprised T2-weighted (w) standard 2D sequences with and without fat saturation (FS) and T1-w unenhanced 2D sequences with and without FS (including in-phase/opposed-phase technique). T1-w 3D sequences with FS were acquired in breath-hold technique before and during arterial and venous/delayed phases following intravenous administration of Gadolinium-containing contrast agents (body weight adapted; manual or automatic injection at approximately 1–2 mL/s flow rate followed by 40 mL saline flush).

Cross-sectional imaging datasets were used for comparison if the examination was performed within one month before or after CEUS examination with renal cortical necrosis diagnosis. Cross-sectional imaging findings were also reviewed by a highly experienced, board-certified radiologist with more than 20 years of experience in radiological imaging in consensus with a second experienced radiologist.

Reference standard. Biopsies were taken on clinical indication only. All patients presented with clinically relevant native kidney or allograft post-transplant dysfunction manifesting as an otherwise unexplained increase in serum creatinine (≥ 1.3 mg/dL), proteinuria (≥ 1 g/day), or primary nonfunction in the early phase after transplantation. Pathologic examinations of biopsy samples taken in patients with renal allografts were performed by experienced nephropathologists. The diagnosis of antibody-mediated rejection was based on the presence of circulating donor-specific antibodies and significant allograft pathology according to the definitions of the up-to-date Banff classification^{16,17}.

Differentiation from renal vein thrombosis. The differentiation of RCN from renal vein thrombosis (RVT) was evaluated by comparing the following sonographic criteria between these patients with confirmed RCN and RVT (confirmed by surgery and/or cross sectional imaging and/or angiography): reduced echogenicity, loss of corticomedullary differentiation, hypoechoic rim, RI > 1 or not measurable due to hypoperfusion of interlobar arteries, delayed wash-in of contrast agent (> 20 s), total loss of cortical perfusion in CEUS, and enhancement of renal medulla. The begin of arterial phase in CEUS was described in the EFSUMB guideline for CEUS in non-hepatic applications by Sidhu et al. to start between 10 and 20 s (except lungs and liver) and so a cut-off value of 20 s was used to assess the arterial-wash-in of contrast agent as delayed¹⁴. The same specific protocols for renal CEUS available at the time of examination as used for RCN were utilized for CEUS in suspicion of RVT.

Patients with RVT of native or transplant kidneys were identified by a systematic search for CEUS reports on examinations performed between 2009 and 2019. For inclusion, confirmation of the diagnosis of RVT by either contrast-enhanced cross-sectional imaging, intraoperative finding, or angiography was necessary.

Statistical analysis. Continuous variables are reported as median and interquartile range (IQR), and categorical variables are reported as proportion of absolute number (n/N) and percentage.

Categorical variables were compared using the χ^2 test and two-sided Fisher's exact test, and both values are given to evaluate possible uncertainties due to the small study cohort. A two-sided significance level of $\alpha = 0.05$ was defined appropriate to indicate statistical significance. All statistical analyses were performed using the SPSS software (IBM Corp., released 2019. IBM SPSS Statistics for Windows, Version 26.0. Armonk, NY: IBM Corp.).

Results

Study cohort. Overall, our systematic query retrieved a total of 18 patients with suspected RCN. After application of the inclusion and exclusion criteria, the retrospective study cohort consisted of 12 patients ≥ 18 years who underwent CEUS of a native kidney (n = 6) or renal transplant (n = 6) between 2009 and 2019. The reasons for exclusion in the six excluded patients were: RCN was diagnosed as differential diagnosis only, the presumed RCN turned out to be caused by a macrovascular pathology (e.g. RVT) and insufficient data storage (e.g. regarding stored cine loops and images)—respectively in two cases each.

Five of the six patients in the native kidney subcohort were postpartum women. The standardized renal CEUS protocol in our institution included B-mode ultrasound, CCDS, and CEUS. Baseline characteristics of the study patients are demonstrated in Table 1.

Chronic kidney disease was known in seven patients, six of them in the renal transplant cohort: one chronic glomerulonephritis, one status after rapidly progressive glomerulonephritis (RPGN) with vasculitis, two patients with diabetic nephropathy, one terminal renal failure due to shrunken kidneys (atrophic kidneys of unknown etiology), one congenital vesicoureteral reflux, and one autosomal-dominant polycystic kidney disease (ADPKD).

Median serum creatinine was 6.83 mg/dL (IQR, 5.81–8.65 mg/dL). Overall, four patients underwent renal transplant nephrectomy due to cortical necrosis.

US and CEUS findings. Imaging findings are summarized in Table 2. B-mode US findings revealed no renal enlargement in any patient with a median kidney length of 10.45 cm (IQR, 9.43–11.80 cm) and width of

Variable	Proportion
Age (years)	52.5 (38.25–60.5)
Female sex	7/12 (58.33%)
Chronic kidney disease	7/12 (58.33%)
Kidney transplant affected	6/12 (50%)
Postpartum period	5/12 (41.67%)
Oliguria	7/12 (58.33%)
Fever	2/12 (16.67%)
Arterial hypertension	9/12 (75%)
Renal anemia	6/12 (50%)
Secondary hyperparathyroidism	7/12 (58.33%)
Diabetes mellitus	3/12 (0.25%)
Major bleeding	6/12 (50%)
Creatinine (mg/dL)	6.83 (5.81–8.65)

Table 1. Baseline characteristic, comorbidities, and clinical findings in all patients. Continuous variables are given as median (IQR), categorical variables as absolute/total numbers (n/N) and percentages in brackets. RCN denotes renal cortical necrosis, IQR interquartile range.

US signs	
Reduced echogenicity	6/12 (50%)
Loss of corticomedullary differentiation	6/12 (50%)
Length of kidney (cm)	10.45 (9.43–11.80)
Width of kidney (cm)	4.90 (4.53–5.98)
Hypochoic rim	4/12 (33.33%)
Resistance index ^a (n = 10)	0.78 (0.60–0.91)
CEUS signs	
Delayed wash-in of contrast agent (> 20 s)	6/12 (50%)
Reverse rim sign	12/12 (100%)
Maximum nonenhancing rim (mm)	4.5 (3–5.8)
Additional renal infarction	4/12 (33.33%)

Table 2. US and CEUS findings in 12 patients with RCN. Continuous variables are given as median (IQR), categorical variables as absolute/total numbers (n/N) and percentages in brackets. US denotes ultrasound, CEUS contrast-enhanced ultrasound, RCN renal cortical necrosis. ^aEleven patients with available data, while one patient had no measurable RI values.

4.90 cm (IQR, 4.53–5.98 cm). Resistance indices (available in n = 10 patients, not available in n = 1 patient, not measurable in n = 1 patient) were slightly increased in four patients with a median RI of 0.78 (IQR, 0.60–0.91), while only one case showed an RI of 1 and no patient showed RI > 1. A subtle subcapsular hypoechoic rim on B-mode US was only visible in four cases despite use of high-end US in all cases.

On CEUS, six patients had a delayed wash-in of the contrast agent (> 20 s). Furthermore, all 12 patients showed a non-enhanced peripheral rim (reverse rim sign) with subcapsular loss of enhancement in the presence of enhancing medullary pyramids. The necrotic rim had a maximum width of 4.5 mm (IQR, 3–5.8 mm). In four patients, CEUS demonstrated renal infarction in addition to RCN. Follow-up CEUS performed in five patients no later than 2 months after the initial examination demonstrated progression of RCN in one case and improved enhancement of the subcapsular rim in two cases.

An exemplary case illustrating the described imaging findings is presented in Fig. 1. Furthermore, Fig. 2 shows examples of different extents of RCN in CEUS.

Histopathological findings. Overall, a histopathological report was available in seven of the twelve patients (58.3%) included in this retrospective analysis. Six histopathological reports were on renal transplants, and three of them diagnosed cellular rejection. In the other three cases, the diagnoses were: pyelonephritis with ischemic alterations of the cortex, arterial alterations with thrombotic occlusions, and vasculitis. For the only native kidney, for which a histopathological examination was available, the diagnosis was cortical infarction with complete loss of viable cortical tissue. A total of five CD4 immunohistological examinations¹⁷ were performed and were negative in all cases.

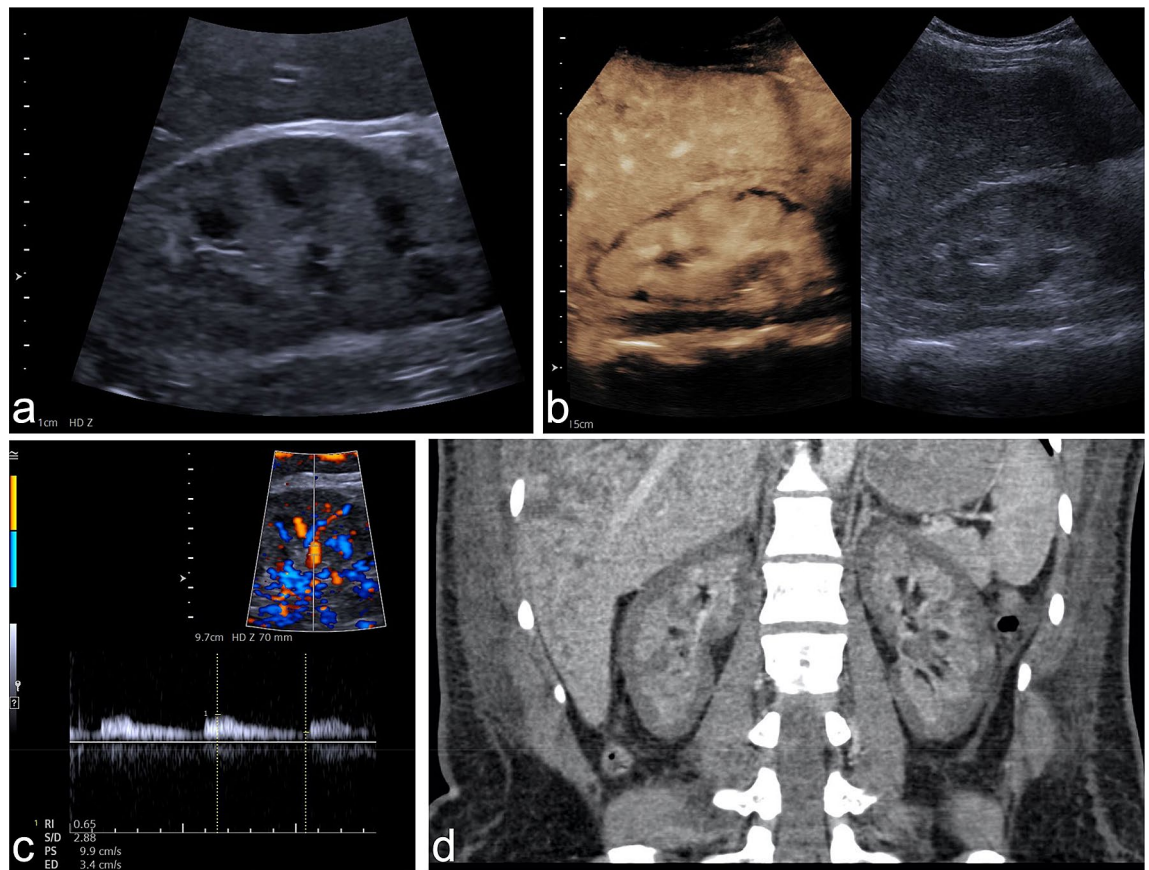


Figure 1. Example of RCN of the native kidney in a 28-year-old woman suffering from massive postpartum bleeding with acute kidney failure and HELLP syndrome. **(a)** B-mode image of the right kidney showing a hypoechoic rim of 3–4 mm. **(b)** CEUS of the right kidney showing a subcapsular loss of contrast enhancement of 3–5 mm. **(c)** Triplex sonography of the right kidney with a PW spectrum of an interlobar artery showing a normal resistance index of 0.65. **(d)** Coronal venous-phase CT scan obtained 14 days before CEUS examination showing a recess of contrast agent measuring up to 6 mm in both kidneys, confirming the diagnosis of RCN. CEUS denotes contrast-enhanced ultrasound, RCN, renal cortical necrosis, HELLP syndrome denotes hemolysis, elevated liver enzymes, low platelets, PW, pulsed-wave Doppler.

Cross-sectional imaging. Overall, nine patients underwent additional multiphase ceCT and two patients additional ceMRI, among them one patient who underwent ceCT and ceMRI (Fig. 3). In two patients, RCN detected by CEUS (one native kidney, one renal transplant) was not detected with ceCT. In these two cases, the maximum necrotic rim measured in CEUS was 2 mm and 3 mm. In the two patients who underwent both CEUS and ceMRI, the two modalities showed consistent findings.

Overall, classical reverse rim sign was visible in four of nine patients in case of ceCT and in one of two patients in case of ceMRI. The cortical rim sign occurred only in two patients, respectively one in ceCT and ceMRI.

Differentiation from renal vein thrombosis. Overall, five patients with RVT in CEUS and surgical, angiographic, or cross-sectional imaging confirmation of the diagnosis were included for assessing the ability of CEUS to differentiate RCN from RVT, which is also characterized by a loss of cortical perfusion, however, with preserved thin subcapsular enhancement (rim sign of vascular compromise)¹⁰. As apparent from the data compiled in Table 3, RI in RVT was always > 1 or not measurable due to significant hypoperfusion of interlobar arteries. Among the eleven RI values available in RCN, only one was not measurable due to hypoperfusion (9.1%) showing therefore strong statistical significance as distinctive feature between RCN and RVT ($p=0.001$ according Fisher's exact test). In the differentiation of RCN from RVT, total loss of cortical perfusion was statistically significant in the chi² test but not in the two-sided Fisher's exact test, whereas enhancing renal medulla (100% in case of RCN, 0% in case of RVT) was found to be statistically significantly different in both tests ($p<0.001$) compared with RCN. Figure 4 provides examples illustrating the different appearance of RVT in CEUS compared to RCN.

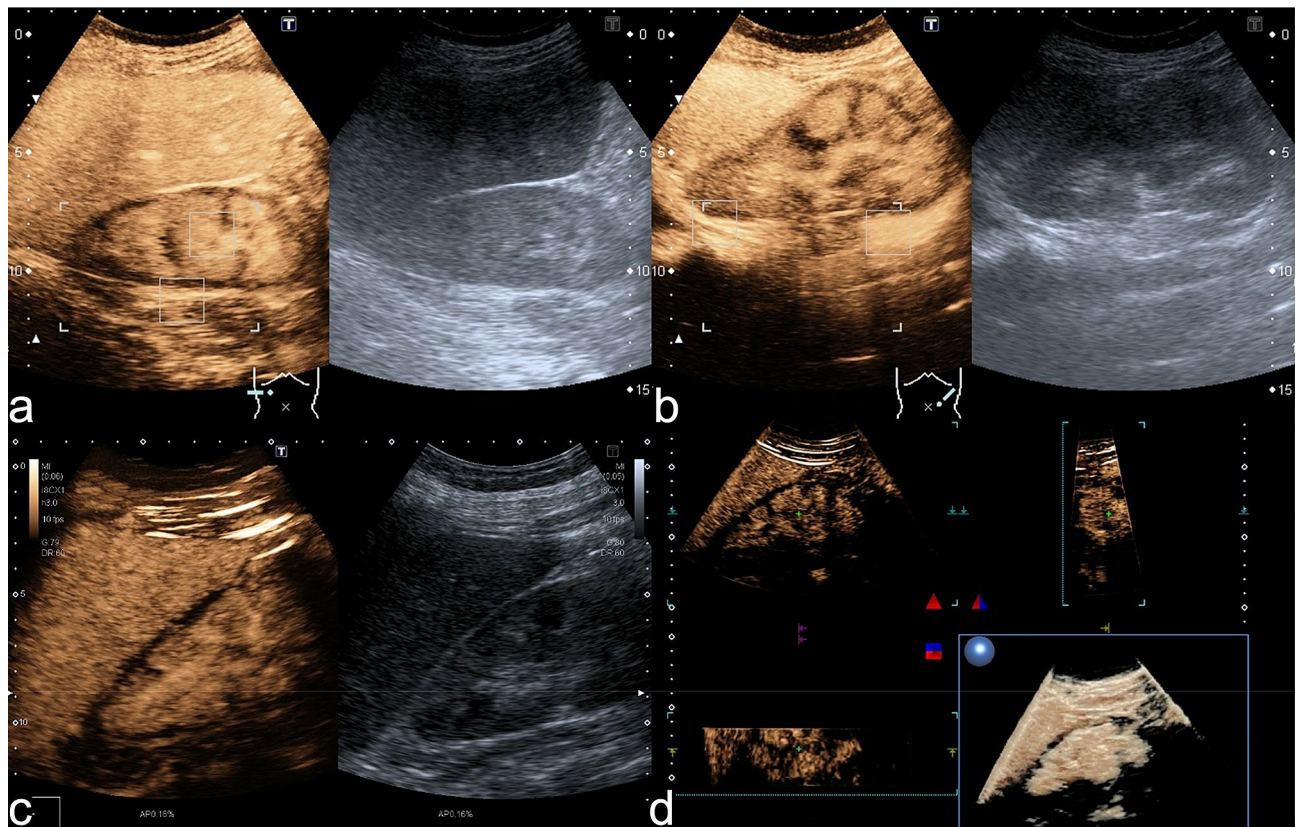


Figure 2. Extent of RCN in CEUS. **(a)** CEUS (0:56 min) of the right kidney in a female patient showing an uninterrupted nonenhancing circular subcapsular rim while B-mode US shows no subcapsular alteration. Note simultaneous enhancement of the medullary pyramids. This pattern is known as the reverse rim sign. **(b)** CEUS (1:20 min) and US image of the left kidney of the same patient consistent with bilateral RCN. **(c)** CEUS (2:15 min) of the right kidney in a different patient showing a subcapsular non-enhancing rim of variable width, especially at the upper pole. **(d)** Same patient as in (c). The 3D rendering of the right kidney during CEUS proves the variation in the width of the nonenhancing subcapsular rim.

Discussion

The main findings of our analysis can be summarized as follows: (1) RI tends to be normal in patients with RCN, (2) real-time CEUS reliably shows the reverse rim sign in RCN, and (3) the combination of CEUS and RI enables differentiation of RCN and RVT in patients with inconclusive CCDS findings.

Imaging findings must always be interpreted in the clinical context and in conjunction with the patient's history: eleven of the twelve patients with RCN in our study had a renal transplant or were postpartum women. All women with postpartum acute renal failure suffered from massive bleeding, which is characteristic of RCN¹⁴.

In 2015, Prakash et al. described RCN to be a disappearing entity in developing countries¹¹, which makes it even more important to keep this rare clinical picture with its typical imaging signs in mind for correct diagnosis. The importance of the clinical background is further corroborated by the fact that RCN needs to be differentiated from RVT: our results show the RI to be a very strong distinctive feature to separate RCN and RVT. Nevertheless, in inconclusive cases, the use of a contrast agent can be expedient. Our results show—at least using the two-sided Fisher's exact test—that total loss of cortical perfusion is not clearly statistically significantly different between the two entities, which is probably driven by the small study cohort. Though, the small number of included cases in the comparative group diagnosing a RVT with CEUS is simply explained by the importance of RI in the diagnosis of RVT making the application of contrast agent in most cases needless. Our results indicate this relationship as well since all included patients in the cohort of RVT had a RI value > 1 or the RI was not measurable due to hypoperfusion (Table 3). Next to imaging features, clinical information according to the patient are relevant: RVT can occur in acute cases in the post-transplant period and should therefore be considered in these cases¹⁸. Furthermore, CEUS needs specialized examiners, who are not always available—therefore, a rational use of CEUS in patients with suspected RVT needs to take into account that emergency surgery should not be delayed highlighting the value of CCDS and RI assessment. Nevertheless—showing high importance in macrovascular problems as RVT—a normal RI value should be considered in consensus with contrast-enhanced imaging when suspected RCN, since our results show B-mode sonography assessing reduced echogenicity (50%), loss of corticomedullary differentiation (50%) and hypoechoic rim (33.33%) not to be reproducible in all included patients (Table 2).

External validation of the imaging pattern of RCN in CEUS is very rare. In the largest cohort of five patients with renal transplant reported so far, the investigators described similar results as in our study including an

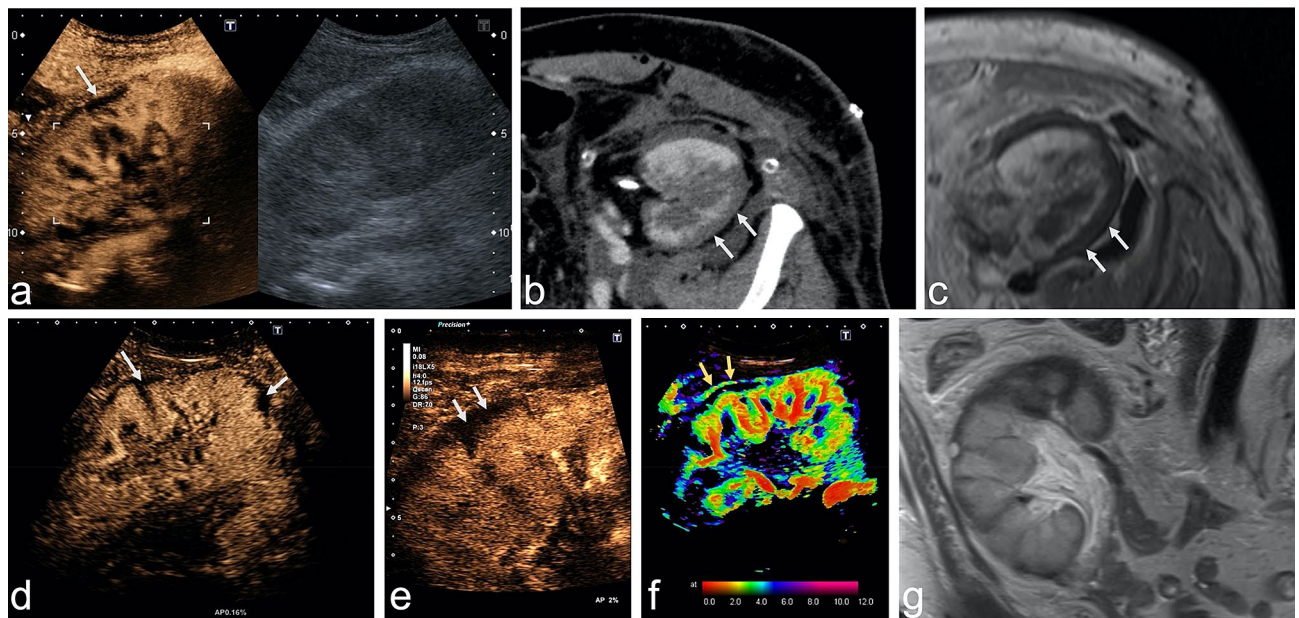


Figure 3. Comparison of modalities in the examination of a kidney transplant with suspected RCN. Upper row: Case showing partial RCN in a renal transplant in a 51-year-old man with end-stage renal failure due to shrunken native kidneys. (a) CEUS (0:59 min) and B-mode US of the renal transplant showing typical reverse rim sign with partial loss of enhancement in subcapsular cortex. (b,c) CeCT (b) and ceMRI (c) showing the hypoenhanced rim of the renal cortex in the transverse plane. Lower row: A case of RCN in a 54-year-old woman with renal transplant. (d) CEUS (1:13 min) using a convex multifrequency probe clearly identifies the reverse rim sign as a nonenhanced rim in the superficial cortex and lower pole (arrows). (e) Increased spatial resolution by use of a linear probe, which is important for second look if CEUS with convex probe shows inconclusive findings. (f) Parametric arrival time imaging of CEUS depicts arterial inflow in interlobar arteries and cortex within 4 s (red and green). Arrows indicate the so-called cortical rim sign with preserved blood supply by capsular arteries (arrows). (g) Coronal T2w MR image confirms the cortical structure defect and moreover shows cortical perfusion deficit at the upper pole of the renal transplant. RCN denotes renal cortical necrosis; CEUS, contrast-enhanced ultrasound; ceCT, contrast-enhanced computed tomography; ceMRI, contrast-enhanced magnetic resonance imaging.

B-mode US signs	RCN (n = 12)	RVT (n = 5)	<i>p</i> (chi ²)	<i>p</i> (two-sided Fisher's exact test)
Reduced Echogenicity	6/12 (50.0%)	0/5 (0%)	0.049	0.102
Loss of corticomedullary differentiation	6/12 (50.0%)	2/5 (40.0%)	0.707	1.000
Hypochoic rim	4/12 (33.3%)	0/5 (0%)	0.140	0.261
Resistance index > 1 or not measurable due to hypoperfusion	1/11 ^a (9.1%)	5/5 (100%)	<0.001	0.001
CEUS signs				
Delayed cortical enhancement	6/12 (50%)	4/5 (80.0%)	0.252	0.338
Total loss of cortical perfusion	0/12 (0%)	2/5 (40.0%)	0.020	0.074
Enhancement of renal medulla	12/12 (100%)	0/5 (0%)	<0.001	<0.001

Table 3. Comparison of B-mode US and CEUS findings in RCN and RVT. A *p*-value < 0.05 indicating statistical significance is marked bold. Continuous variables are given as median (IQR), categorical variables as absolute/total numbers (n/N) and percentages in brackets. RCN denotes renal cortical necrosis, RVT renal vein thrombosis, US denotes ultrasound, CEUS denotes contrast-enhanced ultrasound. ^aMissing image data in one patient.

unenhanced subcapsular cortical band and RI not > 1 in all patients¹⁵. This typical enhancement pattern was also described by Álvarez Rodríguez et al. in two patients and by McKay in a case of bilateral RCN^{19,20}. These studies and our results consistently show that the reverse rim sign¹⁰ is adequately detected by CEUS. The reverse rim sign reflects loss of subcapsular enhancement (Fig. 3a–e, arrows) with preserved medullary enhancement and must be differentiated from the thin cortical rim sign (Fig. 3f, arrows) reflecting preserved supply by capsular arteries. Therefore, CEUS reliably reproduces the classical radiologic signs of RCN which are classically assessed in ceCT¹⁰. Evidence concerning MRI is much thinner, but was described to be comparable to CT²¹, what could be confirmed in the two patients in our study who underwent ceMRI as visualized in Fig. 3c + g.

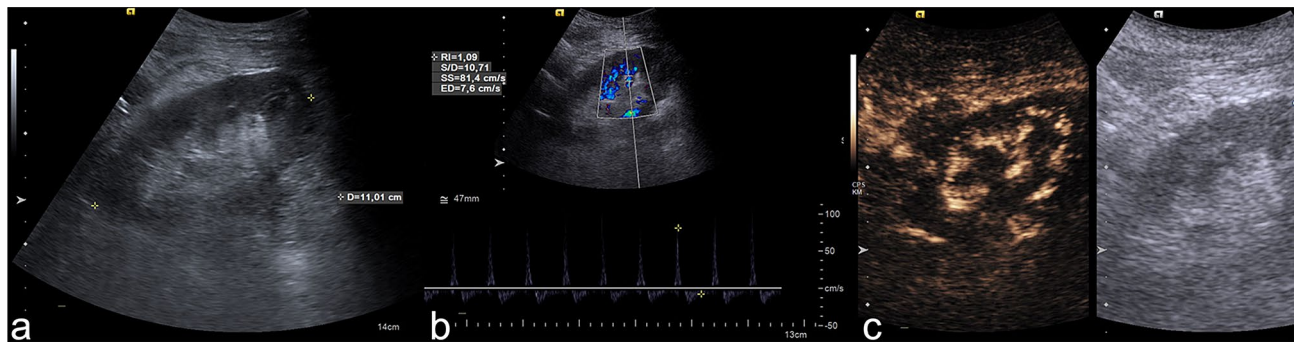


Figure 4. Delimitation of RVT compared to RCN. CEUS examination of a 55-year-old man with renal vein thrombosis. **(a)** The B-mode image shows signs of poor corticomedullary differentiation. **(b)** The pulsed wave (PW) spectrum shows triphasic flow with a resistance index of 1.1, suggesting disturbed venous outflow. **(c)** CEUS (after 50 s) shows no contrast enhancement (indicating loss of microcirculation) of the renal cortex and medullary pyramids. In the cine loop, a pulse-synchronous “pushing” of the microbubbles in the interlobar arteries is visible without cortical enhancement. RVT denotes renal vein thrombosis; CEUS, contrast-enhanced ultrasound, PW, pulsed wave Doppler sonography, RCN, renal cortical necrosis.

Furthermore, there is an ongoing debate about administration of Gadolinium containing contrast agents in patients with kidney disease which is suspected to cause nephrogenic systemic fibrosis (NSF)—which Weinreb et al. summarized to be very low²². Therefore, they recommend to balance rarely occurring NSF and potentially delayed diagnosis against each other²².

In our analysis, enhancement of the renal medulla was absent in all patients with RVT while it was present in all patients with RCN. Thus, the combination of RI and presence versus absence of medullary enhancement may distinguish between RCN and RVT. Since the absent medullary perfusion as a qualitative parameter showed high statistical significance of $p < 0.001$ (Table 3), it suggests that quantitative evaluation of renal perfusion might not be necessary in clinical practice to differentiate RCN from RVT.

Our study patients had conspicuously high mean serum creatinine levels of 6.83 mg/dL (IQR, 5.81–8.65 mg/dL) as indicators of renal failure. Therefore, CEUS is a suitable imaging method in patients with acute loss of kidney function since, unlike iodine-based contrast agents used in ceCT, ultrasound contrast agent is not nephrotoxic^{23–25}. Therefore, CEUS is also suitable for repeat follow-up examinations without a risk of nephrogenic side effects or possible adverse effects of cumulated radiation exposure.

In our study, only 33.33% of the included patients with RCN showed the hypoechoic rim in B-mode ultrasound—although high-end ultrasound machines were used—underlining the need for contrast medium administration in order to diagnose RCN.

In the CEUS follow-up of two patients in our cohort, regression of necrotic areas was observed, indicating that these were cases of incomplete/patchy RCN with the potential of recovery^{4,6}. Although partial recovery of renal function has been discussed for such cases before⁴, there was no restoration of renal function in these two patients of our cohort. A similar course was described by Wieler and Hansmann in a case report of bilateral RCN in a 31-year-old patient with recovery of renal perfusion in CEUS follow-up while retention parameters continued to be elevated²⁶.

Furthermore, studies investigating focal renal lesions in both native kidneys and renal transplants found CEUS to have higher spatial and temporal resolution than ceCT and ceMRI^{27,28}. Since higher resolution also helps in detecting diffuse pathology—especially in renal transplants due to the lower penetration depth in US—CEUS has an important role in these patients. Another important issue are the contrast agents used with different imaging modalities. The microbubbles used for CEUS are strictly intravascular, allowing evaluation whole organ perfusion including microcirculation²⁹. This constitutes an advantage for CEUS over both CT and MRI since iodinated and gadolinium-based contrast media are not purely intravascular²⁹—which could be especially important when assessing necrotic parenchyma.

Limitations

We retrospectively analyzed CEUS findings obtained in a small cohort of patients. Since we use a standardized CEUS protocol for clinical examinations in our department, a prospective study design would not have made much of a difference. Furthermore, a retrospective study design is also reasonable given the rareness of the entity investigated. Finally, we used strict inclusion criteria and required a reference standard—either ceCT, ceMRI, CEUS follow-up, or biopsy—for confirmation of the diagnosis.

Conclusion

Real-time CEUS is a suitable imaging modality for identifying the reverse rim sign in patients with suspected partial RCN, especially when RI values and B-mode US findings are inconclusive. The use of a nonnephrotoxic contrast agent with visualization of renal microvascularization allows evaluation of the entire kidney and use of CEUS for repeat short-term follow-up examinations without a risk of adverse effects on renal function. In combination with RI, CEUS has the potential to differentiate RCN from RVT, which is characterized by complete loss of medullary enhancement.

Received: 18 October 2020; Accepted: 6 January 2021

Published online: 21 January 2021

References

- Prakash, J. *et al.* Decreasing incidence of renal cortical necrosis in patients with acute renal failure in developing countries: a single-centre experience of 22 years from Eastern India. *Nephrol. Dial. Transplant.* **22**, 1213–1217 (2007).
- Malhotra, A. Acute kidney injury (AKI). *Geriatr. Trauma Acute Care Surg.* https://doi.org/10.1007/978-3-319-57403-5_39 (2017).
- Fogo, A. B., Lusco, M. A., Najafian, B. & Alpers, C. E. AJKD atlas of renal pathology: cortical necrosis. *Am. J. Kidney Dis. Off. J. Natl. Kidney Found.* **67**, e27–e28 (2016).
- Prakash, J. *et al.* Spectrum of renal cortical necrosis in acute renal failure in eastern India. *Postgrad. Med. J.* **71**, 208–210 (1995).
- Rodríguez, P. M. *et al.* Cortical necrosis: an uncommon cause of acute renal failure with a very poor outcome. *Nefrología (English Ed.)* **37**, 339–341 (2017).
- Beji, S. *et al.* Acute renal cortical necrosis in pregnancy: clinical course and changing prognosis. *Néphrol. Théor.* **13**, 550–552 (2017).
- Frimat, M. *et al.* Renal cortical necrosis in postpartum hemorrhage: a case series. *Am. J. Kidney Dis. Off. J. Natl. Kidney Found.* **68**, 50–57 (2016).
- Regine, G., Stasolla, A. & Miele, V. Multidetector computed tomography of the renal arteries in vascular emergencies. *Eur. J. Radiol.* **64**, 83–91 (2007).
- Chen, F., Alexander, L. & Caserta, M. Reverse rim sign on CEUS. *Abdom. Radiol.* **45**, 255–256 (2020).
- Dyer, R. B., Chen, M. Y. & Zagoria, R. J. Classic signs in uro-radiology. *Radiogr. Rev. Publ. Radiol. Soc. North Am. Inc.* **24**, S247–S280 (2004).
- Prakash, J. *et al.* Renal cortical necrosis is a disappearing entity in obstetric acute kidney injury in developing countries: our three decade of experience from India. *Ren. Fail.* **37**, 1185–1189 (2015).
- Akbar, S. A. *et al.* Complications of renal transplantation. *Radiographics* **25**, 1335–1356 (2005).
- Granata, A. *et al.* Renal transplant vascular complications: the role of Doppler ultrasound. *J. Ultrasound* **18**, 101–107 (2015).
- Sidhu, P. S. *et al.* The EFSUMB guidelines and recommendations for the clinical practice of contrast-enhanced ultrasound (CEUS) in non-hepatic applications: update 2017 (long version). *Ultraschall Med.* **39**, e2–e44 (2018).
- Fernandez, C. *et al.* Diagnosis of acute cortical necrosis in renal transplantation by contrast-enhanced ultrasound: a preliminary experience. *Ultraschall Med. Eur. J. Ultrasound* **34**, 340–344 (2012).
- Haas, M. *et al.* Banff 2013 meeting report: inclusion of C4d-negative antibody-mediated rejection and antibody-associated arterial lesions. *Am. J. Transplant.* **14**, 272–283 (2014).
- Roufosse, C. *et al.* A 2018 reference guide to the Banff classification of renal allograft pathology. *Transplantation* **102**, 1795–1814 (2018).
- Adani, G. L. *et al.* Risk factors for graft loss due to acute vascular complications in adult renal transplantation using grafts without vascular anomalies. *Transplant. Proc.* **51**, 2939–2942 (2019).
- Álvarez Rodríguez, S. *et al.* The usefulness of contrast-enhanced ultrasound in the assessment of early kidney transplant function and complications. *Diagnostics (Basel, Switzerland)* **7**, 53 (2017).
- McKay, H., Ducharlet, K., Temple, F. & Sutherland, T. Contrast enhanced ultrasound (CEUS) in the diagnosis of post-partum bilateral renal cortical necrosis: a case report and review of the literature. *Abdom. Imaging* **39**, 550–553 (2014).
- Jeong, J. Y. *et al.* MR findings of renal cortical necrosis. *J. Comput. Assist. Tomogr.* **26**, 232–236 (2002).
- Weinreb, J. C. *et al.* Use of intravenous gadolinium-based contrast media in patients with kidney disease: consensus statements from the American college of radiology and the national kidney foundation. *Radiology* **298**, 202903. <https://doi.org/10.1148/radio.1.20202903> (2020).
- Piscaglia, F. & Bolondi, L. The safety of Sonovue in abdominal applications: retrospective analysis of 23188 investigations. *Ultrasound Med. Biol.* **32**, 1369–1375 (2006).
- Tang, C. *et al.* Safety of sulfur hexafluoride microbubbles in sonography of abdominal and superficial organs: retrospective analysis of 30,222 cases. *J. Ultrasound Med.* **36**, 531–538 (2017).
- Tao, S. M. *et al.* Contrast-induced nephropathy in CT: incidence, risk factors and strategies for prevention. *Eur. Radiol.* **26**, 3310–3318 (2016).
- Wieler, J. L. & Hansmann, A. Renale kortikale Nekrose: Verlaufskontrollen mittels kontrastmittelunterstütztem Ultraschall (CEUS). *Rofö* **188**, 1070–1072 (2016).
- Olson, M. C., Abel, E. J. & Mankowski Gettle, L. Contrast-enhanced ultrasound in renal imaging and intervention. *Curr. Urol. Rep.* **20**, 73 (2019).
- Harvey, C. J. *et al.* Role of US contrast agents in the assessment of indeterminate solid and cystic lesions in native and transplant kidneys. *Radiogr. Rev. Publ. Radiol. Soc. North Am.* **35**, 1419–1430 (2015).
- Greis, C. Ultrasound contrast agents as markers of vascularity and microcirculation. *Clin. Hemorheol. Microcirc.* **43**, 1–9 (2009).

Acknowledgements

The authors thank Ms. Bettina Herwig for language editing of the manuscript.

Author contributions

P.S. and M.H.L. conceived the study design and drafted the manuscript. P.S., T.F. and M.H.L. analyzed and interpreted the data. All authors revised the manuscript critically for important intellectual content and gave final approval of the manuscript submitted.

Funding

Open Access funding enabled and organized by Projekt DEAL.

Competing interests

Paul Spiesecke reports no conflict of interest. Frédéric Münch reports no conflict of interest. Thomas Fischer reports having received consultancy honoraria from Bracco and Canon Medical Imaging. Bernd Hamm reports having received consultancy honoraria from Canon Medical Imaging. Markus H. Lerchbaumer reports having received consultancy honoraria from Siemens Healthineers.

Additional information

Correspondence and requests for materials should be addressed to M.H.L.

Reprints and permissions information is available at www.nature.com/reprints.

Publisher's note Springer Nature remains neutral with regard to jurisdictional claims in published maps and institutional affiliations.



Open Access This article is licensed under a Creative Commons Attribution 4.0 International License, which permits use, sharing, adaptation, distribution and reproduction in any medium or format, as long as you give appropriate credit to the original author(s) and the source, provide a link to the Creative Commons licence, and indicate if changes were made. The images or other third party material in this article are included in the article's Creative Commons licence, unless indicated otherwise in a credit line to the material. If material is not included in the article's Creative Commons licence and your intended use is not permitted by statutory regulation or exceeds the permitted use, you will need to obtain permission directly from the copyright holder. To view a copy of this licence, visit <http://creativecommons.org/licenses/by/4.0/>.

© The Author(s) 2021